Journal of Experimental Botany, Vol. 74, No. 6 pp. 1974–1989, 2023
https://doi.org/10.1093/jxb/erac519 Advance Access Publication 28 December 2022

RESEARCH PAPER

Differences in foliar phosphorus fractions, rather than in cell-specific phosphorus allocation, underlie contrasting photosynthetic phosphorus use efficiency among chickpea genotypes

Zhihui Wen[1,2], Jiayin Pang[3,4,*], Xiao Wang[2,3], Clément E. Gille[2], Axel De Borda[2,5], Patrick E. Hayes[2], Peta L. Clode[2,6], Megan H. Ryan[3,4], Kadambot H. M. Siddique[3,4], Jianbo Shen[1,*] and Hans Lambers[1,2,3]

[1] Department of Plant Nutrition, College of Resources and Environmental Sciences; National Academy of Agriculture Green Development; Key Laboratory of Plant-Soil Interactions, Ministry of Education, China Agricultural University, Beijing 100193, China
[2] School of Biological Sciences, The University of Western Australia, Perth, WA 6009, Australia
[3] The UWA Institute of Agriculture, The University of Western Australia, Perth, WA 6009, Australia
[4] UWA School of Agriculture and Environment, The University of Western Australia, Perth, WA 6009, Australia
[5] Agronomy Engineering School of Purpan, 75 Voie du Toec-BP 57611, 31076 Toulouse, France
[6] Centre for Microscopy, Characterisation and Analysis, The University of Western Australia, Perth, WA 6009, Australia

* Correspondence: jbshen@cau.edu.cn or jiayin.pang@uwa.edu.au

Received 4 August 2022; Editorial decision 22 December 2022; Accepted 26 December 2022

Editor: Guohua Xu, Nanjing Agricultural University, China

Abstract

Although significant intraspecific variation in photosynthetic phosphorus (P) use efficiency (PPUE) has been shown in numerous species, we still know little about the biochemical basis for differences in PPUE among genotypes within a species. Here, we grew two high PPUE and two low PPUE chickpea (*Cicer arietinum*) genotypes with low P supply in a glasshouse to compare their photosynthesis-related traits, total foliar P concentration ([P]) and chemical P fractions (i.e. inorganic P (Pi), metabolite P, lipid P, nucleic acid P, and residual P). Foliar cell-specific nutrient concentrations including P were characterized using elemental X-ray microanalysis. Genotypes with high PPUE showed lower total foliar [P] without slower photosynthetic rates. No consistent differences in cellular [P] between the epidermis and mesophyll cells occurred across the four genotypes. In contrast, high PPUE was associated with lower allocation to Pi and metabolite P, with PPUE being negatively correlated with the percentage of these two fractions. Furthermore, a lower allocation to Pi and metabolite P was correlated with a greater allocation to nucleic acid P, but not to lipid P. Collectively, our results suggest that a different allocation to foliar P fractions, rather than preferential P allocation to specific leaf tissues, underlies the contrasting PPUE among chickpea genotypes.

Keywords: Leaf elemental distribution, leaf phosphorus fractions, phosphorus allocation, photosynthetic phosphorus use efficiency, scanning electron microscopy, X-ray microanalysis.

Introduction

Phosphorus (P) plays a central role in many aspects of plant metabolism (Plaxton and Tran, 2011; Dissanayaka *et al.*, 2021) and is one of the nutrients that most frequently limits plant growth and productivity in both natural and agricultural ecosystems (Vitousek *et al.*, 2010; Shen *et al.*, 2011; Lambers, 2022). Photosynthesis commonly declines under P deficiency, since P is involved in a series of cellular processes including energy conservation, metabolic regulation, and signal transduction (Fredeen *et al.*, 1990; Halsted and Lynch, 1996; Stitt *et al.*, 2010;Veneklaas *et al.*, 2012; Raven, 2013a, b; Carstensen *et al.*, 2018). Plant species and even genotypes of a certain species differ in their ability to maintain their photosynthetic activity under P limitation. That is, significant interspecific and intraspecific variation exists for photosynthetic P use efficiency (PPUE, photosynthesis rate per unit foliar P) under low P stress (Halsted and Lynch, 1996; Liao and Yan, 1999; Lambers *et al.*, 2012; Hayes *et al.*, 2018, 2022; Pang *et al.*, 2018; Mo *et al.*, 2019). However, our understanding of the biochemical basis for differences in PPUE among and within species is still in its infancy.

At the species level, two typical hypotheses have been proposed to explain the biochemical basis underlying a high PPUE under low P supply (Lambers *et al.*, 2012; Guilherme Pereira *et al.*, 2018; Hayes *et al.*, 2018; Lambers, 2022). First, as photosynthesis occurs mostly in mesophyll cells and not in common epidermal cells (Lim *et al.*, 2022), it is envisaged that greater allocation of P to the mesophyll may allow a more efficient use of P (hypothesis 1 as shown in Fig. 1). Supporting this hypothesis, such a P-allocation pattern has been demonstrated in monocots and many *Proteaceae* that evolved in severely P-impoverished landscapes (Shane *et al.*, 2004; Hawkins *et al.*, 2008; Conn and Gilliham, 2010; Guilherme Pereira *et al.*, 2018; Hayes *et al.*, 2018, 2019). Despite many *Proteaceae* species showing very low total foliar P concentrations ([P]) in their natural habitats (~0.2 mg g^{-1} dry weight; Hayes *et al.*, 2021), far below the concentration considered adequate for crop growth (2 mg g^{-1} dry weight; Epstein and Bloom, 2005), they exhibit relatively fast rates of photosynthesis per leaf area (e.g. ~20 μmol m^{-2} s^{-1} in *Banksia* species and 15 μmol m^{-2} s^{-1} in *Hakea* species; Denton *et al.*, 2007; Lambers *et al.*, 2012) and exceptionally high PPUE (Wright *et al.*, 2004; Denton *et al.*, 2007; Lambers *et al.*, 2012, 2015; Sulpice *et al.*, 2014). For instance, Lambers *et al.* (2012) reported that the average PPUE value for six *Proteaceae* species was 305 μmol CO_2 g^{-1} P s^{-1}, well above the global average (103 μmol CO_2 g^{-1} P s^{-1}), all measured under field conditions (Wright *et al.*, 2004). The development of X-ray microanalytical mapping has allowed for the visualization and quantification of foliar P distribution at the cellular level (Shane *et al.*, 2004; Ding *et al.*, 2018a; Guilherme Pereira *et al.*, 2018; Hayes *et al.*, 2018, 2019; Ye *et al.*, 2021). Such a technique revealed that many *Proteaceae* from severely P-impoverished soils in southwestern Australia preferentially allocate foliar P to mesophyll cells, rather than epidermal cells (Shane *et al.*, 2004; Hawkins *et al.*, 2008; Guilherme Pereira *et al.*, 2018; Hayes *et al.*, 2018, 2019), but no such pattern was observed in South American species from P-richer habitats, as they may not have had the same evolutionary pressure to increase their P use efficiency (Guilherme Pereira *et al.*, 2018; Hayes *et al.*, 2018). This suggests that preferential allocation of P to photosynthetically active cells (i.e. mesophyll cells) is an important adaptive mechanism to increase PPUE, especially for species that evolved in extremely P-impoverished habitats (Shane *et al.*, 2004; Hawkins *et al.*, 2008; Tsujii *et al.*, 2017; Guilherme Pereira *et al.*, 2018; Hayes *et al.*, 2018, 2019). However, while these findings highlight that differences in cell-specific P allocation contribute to high PPUE at the species level, whether such a cell-specific P-allocation pattern accounts for contrasting PPUE among genotypes within a species remains unexplored.

In addition to differences in cell-specific P allocation, plants can also achieve a relatively high PPUE by adjusting foliar P fractions (hypothesis 2 as shown in Fig. 1) (Stitt *et al.*, 2010; Veneklaas *et al.*, 2012; Sulpice *et al.*, 2014; Lambers *et al.*, 2015; Mo *et al.*, 2019; Hayes *et al.*, 2022). Based on the chemical structure, foliar P compounds can be broadly separated into five distinct fractions: inorganic phosphate (Pi) and four P-containing organic fractions (i.e. metabolite P, lipid P, nucleic acid P, and residual P; Kedrowski, 1983; Hidaka and Kitayama, 2013; Lambers, 2022; Suriyagoda *et al.*, 2023). These P fractions have different functional roles in the biochemical processes of photosynthesis (Stitt *et al.*, 2010;Veneklaas *et al.*, 2012; Lambers *et al.*, 2015; Suriyagoda *et al.*, 2023). Pi maintains a relatively narrow concentration range in the cytosol and is required to export triose phosphates from chloroplasts and for photophosphorylation; any excess Pi is stored in the vacuole, serving as a buffer to maintain a stable Pi concentration in the cytosol (Mimura, 1995; Schachtman *et al.*, 1998;Veneklaas *et al.*, 2012). The foliar metabolite P fraction mainly comprises intermediates of carbon metabolism and various sugar phosphates, such as ADP, ATP, and glucose 6-phosphate, which play key roles in the Calvin–Benson cycle and glycolysis (Lambers, 2022). Lipid P comprises phospholipids, most of which are important components of the plasmalemma and various organelle membranes (Veneklaas *et al.*, 2012; Nakamura, 2017). Nucleic acid P is the largest organic P fraction in leaves (40–60% of total foliar organic P); over 85% of nucleic acid P is contained in RNA (Bieleski, 1973), especially in ribosomal RNA (rRNA), and a high P allocation to rRNA is associated with fast protein synthesis (Raven, 2013b; Lambers, 2022). Finally, the residual P fraction includes phosphorylated proteins and some unidentified residues that cannot be removed with extracting solutions; phosphorylation of proteins is involved in the regulation of various cellular process (Veneklaas *et al.*, 2012; Suriyagoda *et al.*, 2023).

Increasing evidence shows that to achieve relatively fast rates of photosynthesis with high PPUE requires a delicate balance in investment among foliar P fractions (Stitt *et al.*, 2010; Hidaka and Kitayama, 2013; Zhang *et al.*, 2021; Hayes *et al.*, 2022). For instance, some plants suffering from P deficiency can decrease their overall requirement for foliar P by reducing investment in non-metabolite P fractions (e.g. nucleic acid P and lipid P) to different degrees and thus buffering the direct P-restriction of photosynthesis (Warren, 2011; Hidaka and Kitayama, 2013; Mo *et al.*, 2019; Zhang *et al.*, 2021; Han *et al.*, 2022). Lipid remodeling is an essential adaptation mechanism to cope with P starvation in many species (Tjellstrom *et al.*, 2008; Nakamura *et al.*, 2009; Jeong *et al.*, 2017; Tawaraya *et al.*, 2018). Significant replacement of phospholipids (lipid P) by P-free lipids (such as sulfolipids and galactolipids) allows plants to reduce total foliar [P], without compromising a relatively rapid photosynthetic rate (Lambers *et al.*, 2012; Veneklaas *et al.*, 2012; Hidaka and Kitayama, 2013). Overall, these findings suggest that optimized P allocation among foliar P fractions confers a high PPUE under low-P supply at the species level. However, whether and how variation in P allocation to foliar P fractions contributes to contrasting PPUE values among genotypes within a species remains largely unknown.

Chickpea (*Cicer arietinum*) is the third most widely grown grain legume globally, after common bean (*Phaseolus vulgaris*) and cowpea (*Vigna unguiculata*) (FAO, 2020). It is an important source of protein for millions of people and plays a crucial role in food security in developing countries (Jukanti *et al.*, 2012; Varshney *et al.*, 2019). Phosphorus deficiency is one of the major constraints for chickpea production, particularly in low-input agroecosystems (Srinivasarao *et al.*, 2006). Breeding and selecting for chickpea genotypes with high P use efficiency (including high PPUE) is thus a promising strategy to sustainably increase chickpea productivity (Cong *et al.*, 2020). A recent study found considerable genotypic variation in PPUE (170–437 μmol CO_2 g^{-1} P s^{-1}) in a large set of chickpea germplasm under low-P supply (Pang *et al.*, 2018). However, the biochemical basis for differences in PPUE among chickpea genotypes remains unclear. To examine this, we studied four chickpea genotypes with contrasting PPUE in a controlled glasshouse experiment with low P supply. Foliar traits associated with photosynthetic capacity, P fractions and cell-specific P allocation were determined. The study aimed to explore (i) whether and how variation in foliar cell-specific P allocation contributes to contrasting PPUE among chickpea genotypes, and (ii) whether and how the allocation pattern to foliar P fractions accounts for differences in PPUE among chickpea genotypes (Fig. 1).

Materials and methods

Plant material and growing conditions

The experiment was conducted with a single-factorial randomized block design. Four chickpea genotypes contrasting in PPUE were selected, based on results of Pang *et al.* (2018), who reported substantial genotypic variation in PPUE under a low-P supply across 100 chickpea genotypes. The selected genotypes comprised two high-PPUE genotypes (ICC12037, ICC5613) and two low-PPUE genotypes (ICC16524, ICC6877) (see Supplementary Table S1 for detailed information on each genotype).

A loamy clay soil was obtained from the top 15 cm layer of a field paddock at Cunderdin, Western Australia (31.64°S, 117.24°E). The soil was air-dried and passed through a 2-mm sieve. The field soil was mixed with sterilized washed river sand (1:9, soil: river sand) to decrease soil P bioavailability. The soil mixture had a pH of 7.1 (1: 2.5, soil: 10 mM $CaCl_2$), 2.5 mg kg^{-1} resin-P (Sibbesen, 1978), 25.8 mg kg^{-1} total-P, 0.2 mg kg^{-1} ammonium-N, 0.2 mg kg^{-1} nitrate-N, 47.1 mg kg^{-1} Colwell potassium (Colwell, 1965; Rayment and Higginson, 1992), and 8.7 g kg^{-1} organic carbon (Heanes, 1984). Each pot was filled with 2.4 kg of the air-dried soil mixture. To ensure that the supply of other nutrients was adequate for plant growth, the soil mixture was supplemented with basal nutrients at the following rates (mg kg^{-1}): $Ca(NO_3)_2{\cdot}4H_2O$, 94.8; NH_4Cl, 14.3; K_2SO_4, 272; EDTA-FeNa, 37.6; $MnSO_4{\cdot}H_2O$, 12.3; $ZnSO_4{\cdot}7H_2O$, 8.86; $CuSO_4{\cdot}5H_2O$, 1.95; and $Na_2MoO_4{\cdot}2H_2O$, 1.01. Nine seeds were sown per pot and inoculated with ~2 g of peat-based Group N rhizobium (New Edge Microbials, North Albury, NSW, Australia). Seedlings were thinned to three plants per pot 14 d after sowing (DAS). There were four replicates per genotype and five pots per replicate (80 pots in total). All pots within each block were arranged randomly and watered daily with deionized water by weighing to 75% of maximum water holding capacity.

The experiment was conducted from May to July 2019 in a naturally lit glasshouse at The University of Western Australia, Perth, Australia (31.95°S, 115.78°E). The average daily temperature was 22/15 °C (day/night), and the average relative humidity was 65%.

Photosynthesis measurement

Prior to the final harvest (48 DAS), net photosynthetic rates (P_n) were measured on young fully expanded leaves on primary branches using portable photosynthesis equipment with a red/blue LED light source (LI-6400XT, Li-Cor Biosciences, Lincoln, NE, USA). Photosynthetic photon flux density at the leaf surface was 1500 μmol m^{-2} s^{-1}, ambient CO_2 concentration of the incoming gas was 400 μmol mol^{-1}, flow rate was 500 μmol s^{-1}, block temperature was 25 °C, and relative humidity was maintained at 50–70%. The leaves used for photosynthesis measurements were sampled, with the projected leaf area measured at 300 dpi using a flatbed scanner (Epson Perfection v850 pro, Tokyo, Japan) and analysed using WinRhizo 2009 software (Regent Instruments Inc., Quebec, Canada), followed by drying at 70 °C for 72 h to constant weight. Leaf mass per area (LMA) of the leaves used for photosynthesis measurement was calculated as the ratio of leaf dry weight (DW) to leaf area. Mass-based photosynthetic rate (A_{mass}, nmol CO_2 g^{-1} s^{-1}) was calculated from the area-based photosynthetic rate (A_{area}, μmol CO_2 m^{-2} s^{-1}) divided by LMA. Photosynthetic phosphorus use efficiency (PPUE, μmol CO_2 g^{-1} P s^{-1}) was calculated as the ratio of A_{mass} to the corresponding foliar [P] (DW basis).

Plant harvest and leaf sampling for cell-specific element analysis and P fractionation

Plants were harvested after P_n measurement (49 DAS). For cellular element analyses, subsamples of young fully expanded leaves similar to those used for P_n measurement were collected, following the method described by Hayes *et al.* (2018) and Ye *et al.* (2021). In brief, small leaf sections (~2 × 3 mm) were cut from either side of the mid-rib, at the middle of the half-leaflet, avoiding any large secondary veins. Each section was then quickly mounted onto an aluminum pin with an optimal cutting temperature compound (Tissue-Tek, Torrance, CA, USA) and plunged into liquid nitrogen. Three sections were collected from two to three leaflets

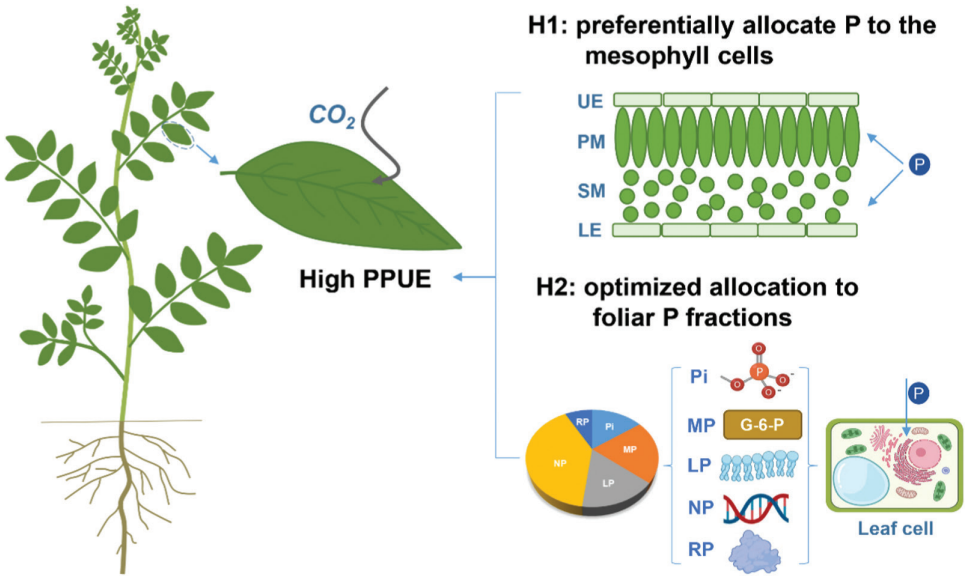

Fig. 1. Conceptual diagram illustrating two potential mechanisms underlying high photosynthetic phosphorus (P) use efficiency (PPUE) in plants. Hypothesis 1 (H1): in response to low P supply, plant species and/or genotypes with high PPUE preferentially allocate the scarcely available P to their mesophyll cells where P is used to sustain photosynthesis, rather than to epidermal cells. Hypothesis 2 (H2): to maintain a relatively high photosynthetic capacity, plant species and/or genotypes with high PPUE show an optimized allocation of foliar P to different chemical fractions. Leaf cell types: LE, lower epidermis; PM, palisade mesophyll; SM, spongy mesophyll; UE, upper epidermis. Foliar P fractions: LP, lipid P; MP, metabolite P; NP, nucleic acid P; Pi, inorganic phosphate; RP, residual P. G-6-P, glucose-6-phosphate. The leaf cross section shown in H1 represents typical leaf anatomy of some dicots, including chickpea. Figure adapted from images created with BioRender.com.

for each plant. All samples were taken back to the laboratory and stored in a dewar filled with liquid nitrogen until cellular element analysis using cryo-scanning electron microscopy. This freezing method is suitable for elemental analysis and quantification of biological samples, because it rapidly immobilizes and preserves elements of interest at the cellular level (McCully *et al.*, 2010; Hayes *et al.*, 2018; Ding *et al.*, 2018a; Ye *et al.*, 2021).

For foliar [P] and P fraction analyses, another subsample of young fully expanded leaves similar to those used for P_n measurement was collected. Leaves from five pots of each replicate were combined into one sample for P fractionation. All leaves were washed with deionized water and quickly wrapped in aluminum foil, and immediately frozen in liquid nitrogen. The samples were kept at −80 °C until freeze-drying for P-fraction analyses.

Cell-specific element analysis by X-ray microanalytical mapping

Frozen specimens were transferred under liquid nitrogen to a cryo-microtome (Leica Ultracut EM UC6 microtome equipped with FC6 cryo-chamber, Leica Microsystem GmbH, Vienna, Austria). To obtain flat and transverse surfaces of frozen leaf samples, leaves were progressively sectioned flat with a microtome, initially on a glass knife in 1 µm, 750 nm, and 500 nm steps, and then finally with fine precision on another glass knife in 250 and 100 nm steps. Specimens were then mounted on a custom-made substage and transferred to a modular high-vacuum coating system (Leica EM MED020) and sputter-coated with 20 nm high purity chromium, without sublimation. After coating, specimens were transferred under vacuum to a field emission scanning electron microscope (Zeiss Supra 55, Oberkochen, Germany), equipped with a Leica VCT100 cryostage and an Oxford X-Max80 SDD X-ray detector interfaced to AZtec software (Oxford Instruments, Abingdon, UK).

Samples were analysed in high-current mode at −150 °C, 15 kV, and 2.0 nA beam current (measured with a Faraday cup). Prior to each map acquisition, the instrument was calibrated using a pure copper standard. Elemental maps were acquired at a resolution of 512 pixels, for >3000 frames with a dwell time of 10 µs per pixel. Drift correction and pulse-pile-up correction were activated. After mapping, measured scanning electron microscopy and energy dispersive spectroscopy data were evaluated using AZtec software. Specifically, quantitative numerical data were extracted from regions of interest (i.e. individual cells) drawn on the element maps. Individual spectra from each pixel within the region of interest were processed and summed to yield concentration data. Details of operations and principles are described elsewhere (Hayes *et al.*, 2018; Ding *et al.*, 2018a).

The chickpea genotypes had very similar leaf anatomy and cell types, including upper epidermis, palisade mesophyll, spongy mesophyll, lower epidermis, bundle sheath, and veins. To contrast cell-specific P allocation between photosynthetic cells and non-photosynthetic cells, the concentrations of P and calcium (Ca) in upper epidermal, palisade mesophyll, spongy mesophyll, and lower epidermal cells were measured by selecting these cells as regions of interest in the elemental maps and quantifying the resulting summed spectra.

Foliar nutrient concentrations and phosphorus fractionation

After harvest, samples of young fully expanded leaves were freeze-dried for 7 d (VirTis Benchtop 'K', New York, USA) before being ground to a fine powder in a vertical ball-mill grinder using plastic vials and ceramic beads (Geno/Grinder 2010; Spex SamplePrep, Metuchen, NJ, USA). Each sample was divided into four subsamples. One subsample (~20 mg) was used to determine total [N] using an elemental analyser (Vario EL III; Elementar, Langenselbold, Germany). A second subsample (~50 mg) was used to measure total [P]; after digestion in a concentrated HNO_3–$HClO_4$ (3:1 v/v) mixture, the P concentrations were determined using the malachite green colorimetric method (Motomizu *et al.*, 1983).

Foliar P was partitioned into inorganic phosphate (Pi) and organic P (lipid P, metabolite P, nucleic acid P, and residual P). A detailed description of the P fractionation procedures is available in previous studies (Yan *et al.*, 2019; Hayes *et al.*, 2022). In brief, a third subsample (~20 mg) was used to measure Pi. The Pi fraction was extracted using acetic acid (modified from Hurley *et al.*, 2010). This subsample was treated with 1 ml of 1% (v/v) cold glacial acetic acid by mechanical shaking (Precellys 24 Tissue Homogenizer; Bertin Instruments, Montigny-le-Bretonneux, France). Then, the homogenate was centrifuged at 4 °C for 15 min at 14 000 *g* to remove debris. The final clear supernatant was transferred to a new tube to determine P concentrations using the malachite green colorimetric method (Motomizu *et al.*, 1983).

Organic P fractions were sequentially extracted following the method adapted from Hidaka and Kitayama (2013). A fourth subsample (~25 mg) was weighed into a 2-ml tube and then extracted three times with 1 ml cold 12:6:1 chloroform: methanol: formic acid (CMF, v/v/v), followed by extraction, three times, with 1.26 ml cold 1:2:0.8 chloroform: methanol: water (CMW; v/v/v). Supernatants from these extractions were transferred and combined into a 10-ml tube, and then 1.9 ml of chloroform-washed water was added, resulting in a biphasic solution with a hydrophilic upper layer (white/transparent) and a hydrophobic lower layer (green), separated by a thin semi-solid interfacial protein layer. The upper aqueous layer and the lower lipid layer were extracted and transferred to two new 25-ml flasks, labeled metabolic P and lipid P, respectively. The lipid P was ready for acid digestion after drying. The remaining interfacial layer was transferred to the metabolic P flask.

The CMF/CMW extracted pellet was dried under vacuum and then extracted with 1 ml of 85% methanol (v/v) to remove dissolved chloroform and methanol. The supernatant was transferred to the metabolic P flask and the pellet dried under vacuum again. Then, this dried pellet was extracted twice with 1 ml cold 5% trichloroacetic acid (TCA, v/v), with horizontal shaking for 1 h at 4 °C. The supernatant was transferred to the metabolic P flask. The metabolic P was ready for acid digestion after drying. Metabolic P represented the sum of the metabolite P and Pi fractions; thus, we subtracted Pi from the sum to obtain the metabolite P.

Finally, the pellet was further extracted three times with 1 ml of 2.5% TCA (v/v) in a heating block at 95 °C for 1 h. The resulting supernatants were transferred to another 25-ml flask for nucleic acid P analysis. The remaining pellet was washed with 2.5% TCA and the washing solution was transferred to another 25-ml flask for residual P analysis.

The flasks containing the four P fractions were evaporated gently in a fume-hood at 50 °C; the determination method of the dried residue of the four P fractions was the same as that of total foliar P. To avoid conversion of P fractions during extraction, all samples were kept on ice, unless otherwise specified. All foliar P fractions are expressed on a dry mass basis. The percentage of each P fraction was calculated from the P fraction concentration and total foliar [P], determined separately by acid digestion. The recovery of the sum of P in the fractions was always >95% of the total [P] measured directly from freeze-dried leaves (Supplementary Table S2).

Data analyses

To determine how genotypes with contrasting PPUE expressed their foliar traits and P fractions at a low P supply, a one-way ANOVA with a randomized block design was performed to examine the genotypic effects on foliar traits, photosynthetic traits, and the concentrations of total foliar nutrients and P fractions using the R package 'AGRICOLAE' (de Mendiburu, 2017). Differences in nutrient concentrations (including P and Ca) among cell types were tested using general linear mixed-effect models, with individual plants included as the random effect (Pinheiro and Bates, 2000). The residuals of each model were visually inspected for heteroscedasticity. In presence of heteroscedasticity, appropriate variance structures were specified if they significantly improved the model based on the Akaike information criterion (Pinheiro and Bates, 2000). Significant differences among genotypes and/or cell types within each genotype were based on Tukey's HSD post-hoc analysis ($P \leq 0.05$). Correlations between PPUE and total foliar [P] and P fractions were assessed by linear regression analysis using the R package 'AGRICOLAE' (de Mendiburu 2017). All statistical analyses were performed using R software Version 4.0.2 (R Development Core Team, 2022).

Results

Foliar photosynthetic capacity and total foliar nutrient concentrations

As expected, we observed significant variation in photosynthetic PPUE among the four chickpea genotypes ($P<0.01$, Fig. 2A). Two genotypes, ICC12037 and ICC5613, showed greater PPUE (341 and 335 μmol CO_2 g^{-1} P s^{-1}) than the other two, ICC16524 and ICC6877 (248 and 238 μmol CO_2 g^{-1} P s^{-1}). The four genotypes had similar area-based and mass-based photosynthetic rates (A_{area} and A_{mass}; Fig. 2B, C), except that ICC16524 had significantly lower A_{area} than the others ($P<0.01$, Fig. 2B). The LMA ranged from 34.3 to 37.6 g m^{-2}; ICC16524 had significantly lower LMA than ICC12037 and ICC6877 ($P<0.01$, Fig. 2D). The two high-PPUE genotypes (ICC12037 and ICC5613) had lower foliar [P] than one of the low-PPUE genotypes (ICC6877) and similar foliar [P] to the other low-PPUE genotype (ICC16524) (Fig. 2E). All genotypes showed similar leaf [N] ($P>0.05$, Fig. 2F). The leaf N:P ratio ranged from 20.7 to 29.8, with ICC6877 (20.7) significantly lower than the other three genotypes ($P<0.01$, Fig. 2G).

Foliar cell-specific nutrient concentrations

Foliar cellular nutrient concentrations differed among cell types (Figs 3, 4; Supplementary Figs S1, S2). Under low P supply, all genotypes showed very low [P] in all cell types, averaging below 10 μmol g^{-1} (Fig. 3A). No consistent difference in cellular [P] occurred between mesophyll and epidermal cells within each genotype (Fig. 3A), indicating no preferential P allocation to leaf photosynthetic cells among genotypes with contrasting PPUE. Interestingly, most Ca was located in the mesophyll cells (both palisade and spongy mesophyll) for all genotypes. The cellular [Ca] of each genotype following the order: palisade mesophyll cells>spongy mesophyll cells>upper epidermal cells>lower epidermal cells (Fig. 3B). Similarly, all genotypes tended to allocate more sulfur to mesophyll cells than to epidermal cells (Supplementary Fig. S1). In contrast, most potassium and magnesium was located in both upper and lower epidermal cells (Supplementary Figs S1, S2). The allocation pattern of chlorine (Cl) tended to be similar among different cell types, with only slight differences in [Cl] between epidermal and mesophyll cells (Supplementary Figs S1, S2).

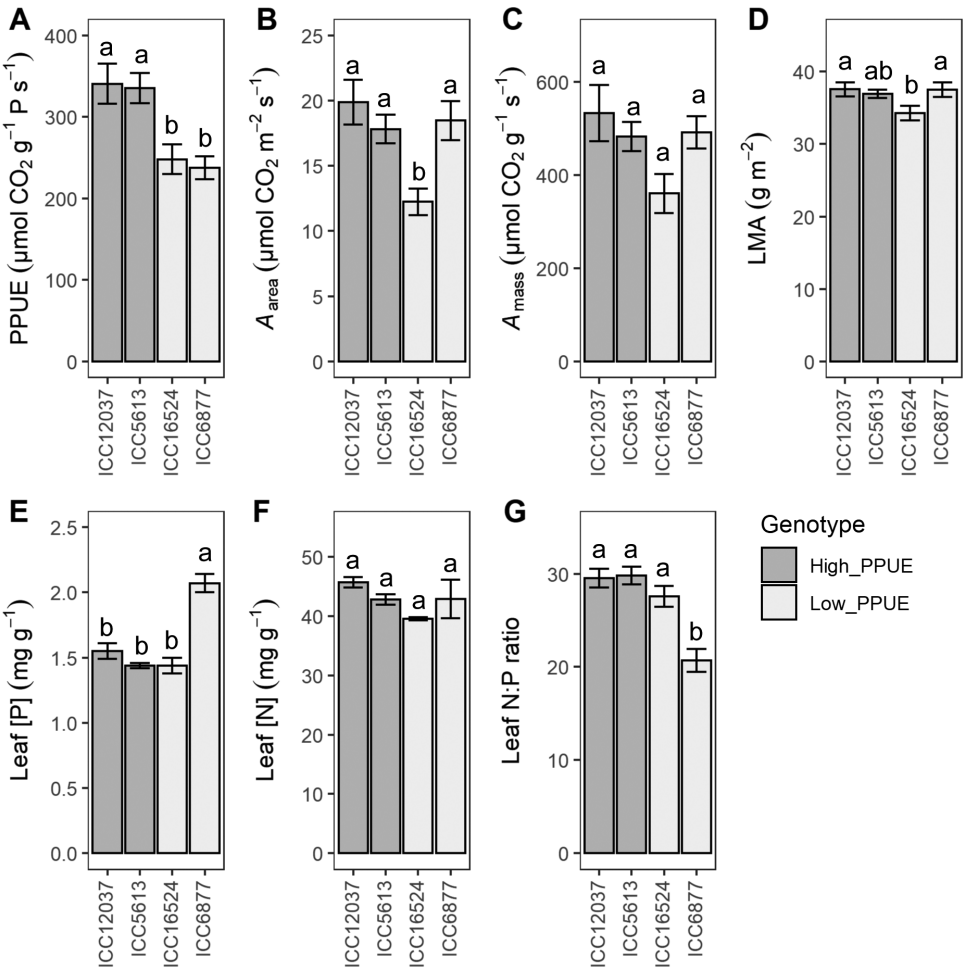

Fig. 2. Bar plots showin photosynthetic phosphorus use efficiency (PPUE)g (A), area-based (B) and mass-based (C) photosynthetic rates (A_{area} and A_{mass}), leaf mass per unit leaf area (LMA; D), leaf phosphorus (P) concentration ([P], E), leaf nitrogen (N) concentration ([N]; F), and leaf N:P ratio (G) for four chickpea genotypes grown in soil with a low P supply. Values are means ±SE (n=4). Different letters indicate significant differences among genotypes within each panel, based on Tukey's post-hoc analysis (P<0.05).

Foliar P fraction concentrations and allocation

The major foliar P fractions of chickpea were inorganic phosphate (Pi), metabolite P, lipid P and nucleic acid P, comprising 99% of the total foliar [P] (Fig. 5), with residual P only a minor component (below 0.01 mg g^{-1}) in all genotypes (Fig. 5E). Similar to total foliar [P], the two high-PPUE genotypes (ICC12037 and ICC5613) had lower [Pi], metabolite [P], and lipid [P] than one of the low-PPUE genotypes (ICC6877) (P<0.01), but no significant differences from the other low-PPUE genotype (ICC16524) (P>0.05; Fig. 5A–C). In contrast, no significant differences in nucleic acid [P] occurred between the high-PPUE and low-PPUE genotypes, except ICC6877 had a greater concentration than ICC16524 (Fig. 5D). The concentrations of four major P fractions were positively correlated with total foliar [P] (all R^2>0.5, P<0.001; Supplementary Fig. S3).

P allocation was expressed as a percentage of total foliar P allocated to each P fraction (Fig. 5). The percentage of each foliar P fraction in each genotype followed the order of nucleic acid P>metabolite P>Pi=lipid P (Fig. 5F–I). Across the four genotypes, nucleic acid P accounted for 39–47% of total foliar [P], metabolite P for 21–25%, Pi for 15–18%, and lipid P for 16–18% (Fig. 5F–I). No significant differences in the percentages of Pi, metabolite P, and lipid P occurred between genotypes; however, the high-PPUE genotypes (ICC12037 and ICC5613) tended to have a greater percentage of nucleic acid P than the low-PPUE genotypes (ICC16524 and ICC6877) (P<0.01; Fig. 5F–I).

Relationships between foliar P fractions and PPUE across chickpea genotypes

Across the four chickpea genotypes, A_{mass} and A_{area} were positively correlated with total foliar [P] and nucleic acid [P] (all P<0.05), but not with the other three major foliar P fractions (all P>0.05; Supplementary Table S3). No significant

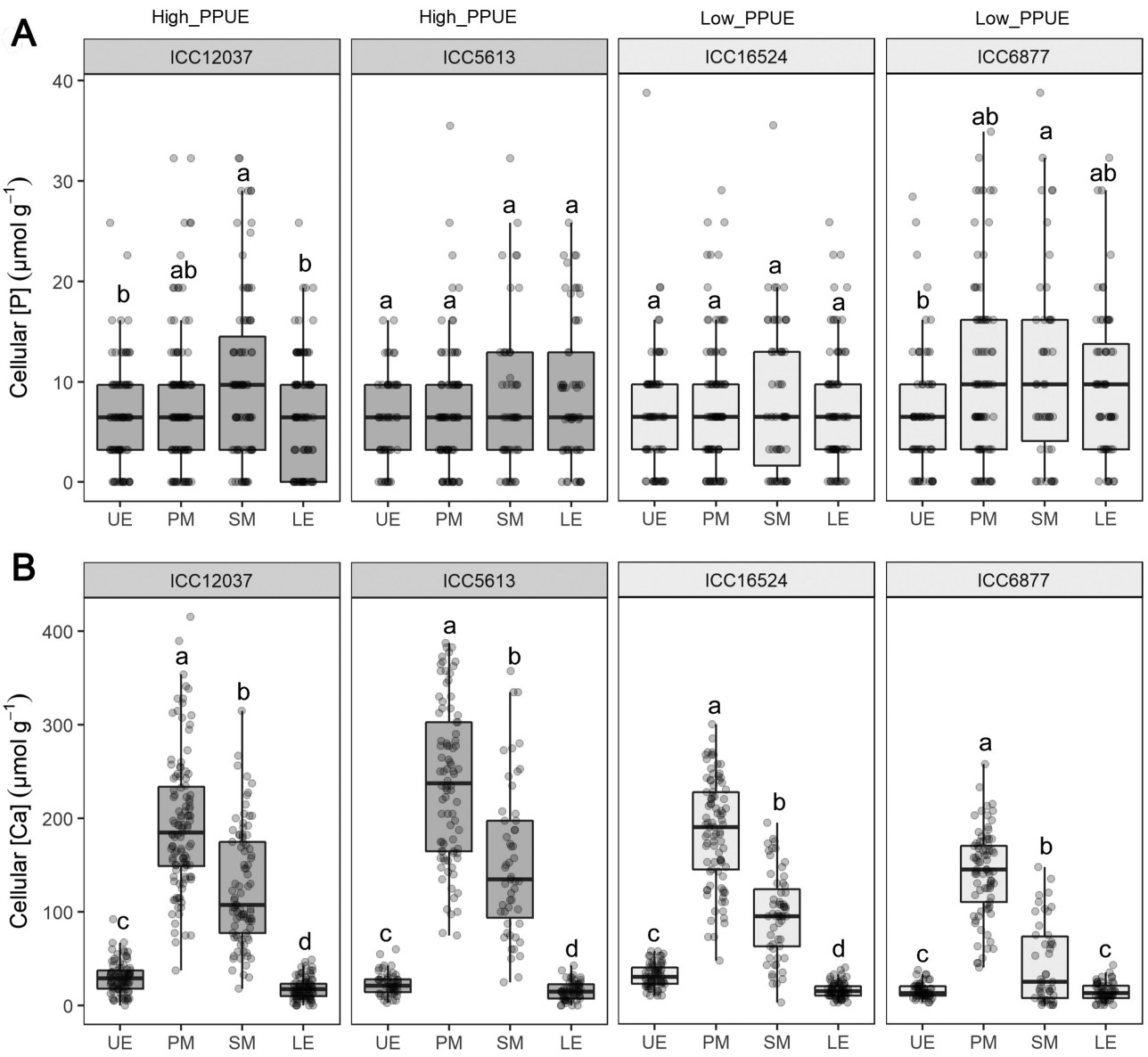

Fig. 3. Box plots showing foliar cell-specific phosphorus (P) concentrations ([P]) (A) and calcium (Ca) concentrations ([Ca]) (B) for four chickpea genotypes grown in soil with a low P supply. The box plots show the medians, 25th, and 75th percentiles, and the whiskers extend to 1.5 times the interquartile range. Data presented beyond whiskers represent outliers. Different letters indicate significant differences among cell types within each panel, based on Tukey's post-hoc analysis (P<0.05). Leaf cell types: LE, lower epidermis; PM, palisade mesophyll; SM, spongy mesophyll; UE, upper epidermis. High_PPUE: genotype with high photosynthetic phosphorus use efficiency (PPUE); Low_PPUE: genotype with low PPUE.

correlation was found between PPUE and the concentrations of the major foliar P fractions (all P>0.05; Fig. 6A–D). In contrast, the allocation pattern of foliar P fractions affected PPUE differently (Fig. 6E–H), with PPUE being positively correlated with the percentage of nucleic acid [P] (R^2=0.56, P<0.001), and negatively with the percentages of [Pi] and metabolite [P] (R^2=0.27, 0.39, respectively), and no correlation with lipid [P] (P>0.05; Fig. 6E–H).

To explore the linkages between nucleic acid P and other P fractions, we determined the correlation of the concentrations and percentages of nucleic acid P with those of other P fractions (Fig. 7). Across the four genotypes, nucleic acid [P] was positively correlated with [Pi], metabolite [P], and lipid [P] (all P<0.05; Fig. 7A–C), while the percentages of nucleic acid [P] was negatively correlated with the percentages of [Pi] and metabolite [P] (all P<0.001; Fig. 7D, E), but not with the percentage of lipid [P] (P>0.05; Fig. 7F). As a result, PPUE was positively correlated with the ratios of nucleic acid P to Pi (R^2=0.40, P<0.01), the ratio of nucleic acid P to metabolite P (R^2=0.51, P<0.01), and the ratio of nucleic acid P to lipid P (R^2=0.37, P<0.05) (Fig. 7C).

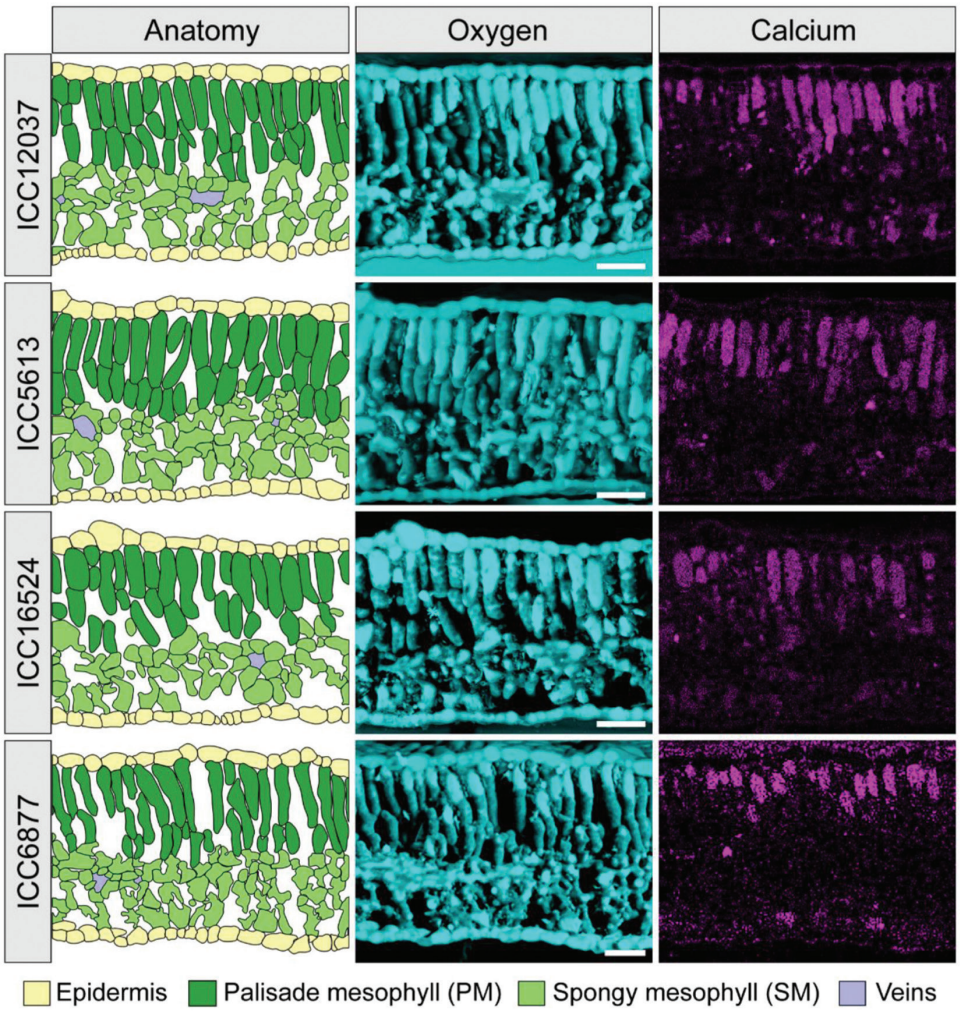

Fig. 4. Representative anatomical schematics and qualitative element maps for four chickpea genotypes grown in soil with a low phosphorus (P) supply. Maps show oxygen (O) and calcium (Ca) distribution in transverse sections of young fully expanded leaves. Element maps were processed to remove background and correct for peak overlaps. The element maps for P are not shown due to a lack of contrast among cell types resulting from very low concentrations. Scale bars: 50 μm.

Discussion

We found significant intraspecific variation in PPUE at low soil P availability among chickpea genotypes, confirming our previous study (Pang *et al.*, 2018). Compared with the low-PPUE genotype ICC6877, those with high PPUE exhibited lower total foliar [P] while maintaining relatively rapid photosynthetic rates, indicating a more economic P use strategy in their leaves. Towards an improved understanding of the biochemical basis of how chickpea exhibited contrasting PPUE at the genotype level, we tested two possible pathways, i.e. optimized P allocation to specific leaf tissues and/or to foliar P fractions, contributing to a greater PPUE among chickpea genotypes (Fig. 1).

Does foliar cell-specific P allocation account for contrasting PPUE among chickpea genotypes?

As photosynthesis occurs in mesophyll cells and not in common epidermal cells (Lim *et al.*, 2022), we hypothesized that preferential allocation of P to the mesophyll would contribute to a high PPUE in chickpea genotypes (H1, as shown in Fig. 1). However, no consistent differences in cellular [P] occurred between mesophyll and epidermal cells across the four chickpea genotypes with contrasting PPUE; thus, we rejected our first hypothesis (H1).

Greater relative allocation of P to mesophyll cells is reported for many monocots (Hodson and Sangster, 1988; Leigh and Tomos, 1993; Williams *et al.*, 1993; Fricke *et al.*, 1994; Karley *et al.*, 2000a, b) and some extremely P-efficient species that evolved in severely P-impoverished habitats (Shane *et al.*, 2004; Hawkins *et al.*, 2008; Guilherme Pereira *et al.*, 2018; Hayes *et al.*, 2018, 2019). According to the conceptual model for foliar P distribution in eudicots proposed by Conn and Gilliham (2010), these species typically allocate P to the epidermis, rather than to mesophyll cells. This model is supported by observations on faba bean (*Vicia faba*; Outlaw *et al.*, 1984), several *Lupinus* species (Treeby *et al.*, 1987; Ding *et al.*, 2018a, b) and rough lemon

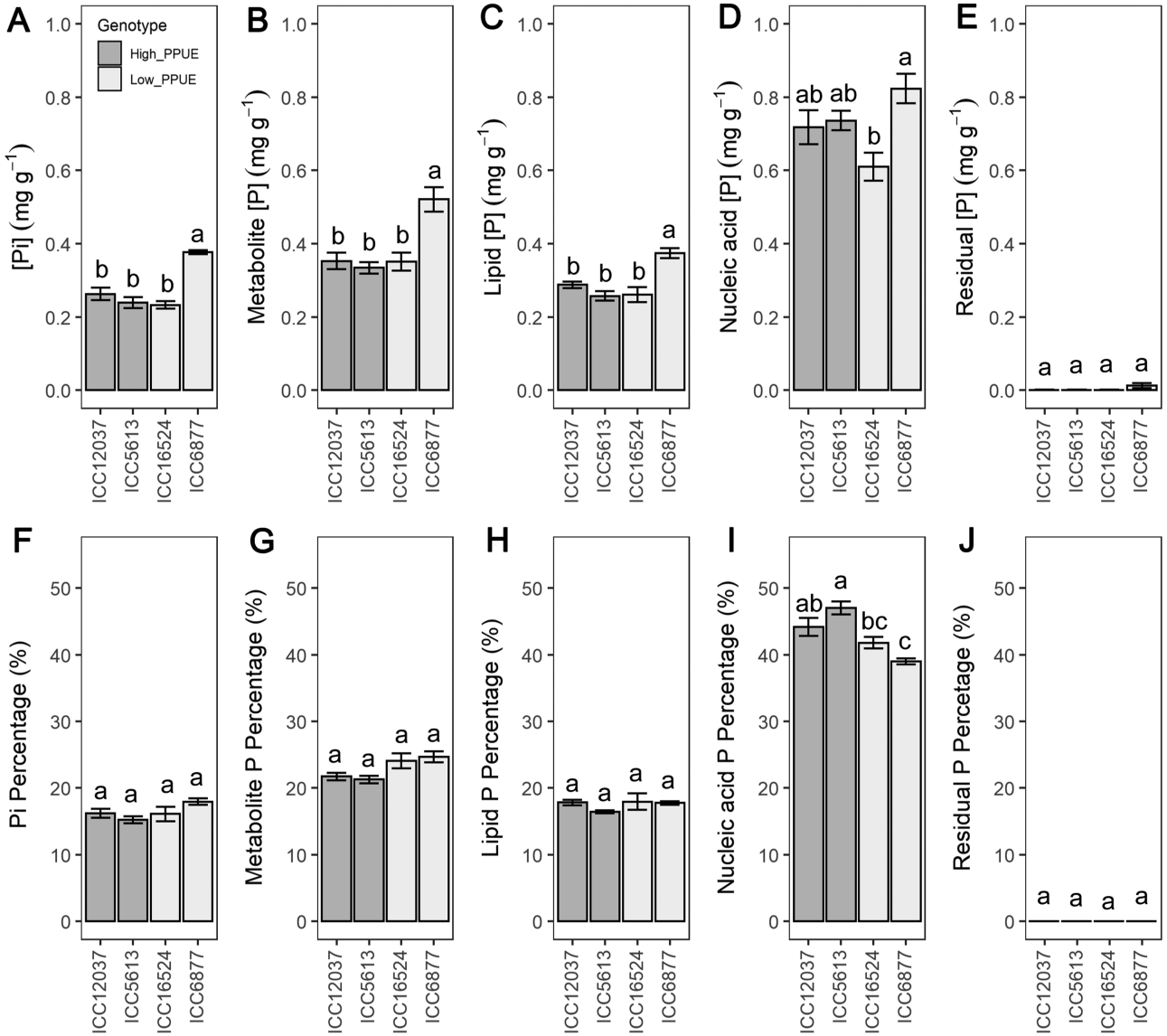

Fig. 5. Bar plots showing the concentrations of foliar phosphorus (P) fractions (A–E) and percentage of each P fraction of the total foliar P concentration (F–J) for four chickpea genotypes grown in soil with a low P supply. Values are means ±SE (n=4). Different letters indicate significant differences among genotypes within each panel, based on Tukey's post-hoc analysis (P<0.05). Pi, inorganic phosphate. High_PPUE: genotype with high photosynthetic phosphorus use efficiency (PPUE); Low_PPUE: genotype with low PPUE.

(*Citrus jambhiri*; Storey and Leigh, 2004) at the species level. Remarkably, this was not the case for chickpea studied here, as all genotypes showed similar [P] across four leaf cell types. Such a P-allocation pattern in chickpea agrees with the findings on some *Proteaceae* species from South America that evolved in relative P-rich soils (Hayes *et al.*, 2018), but is inconsistent with results on *Proteaceae* from southwestern Australia that evolved in extremely P-impoverished soils (Shane *et al.*, 2004; Guilherme Pereira *et al.*, 2018; Hayes *et al.*, 2018). Thus, our study provides further evidence that preferential allocation of P to mesophyll is not common in eudicots, and, to date, is only expressed in some P-efficient eudicot species that evolved in extremely P-impoverished landscapes (Guilherme Pereira *et al.*, 2018; Hayes *et al.*, 2018; Lambers, 2022). Furthermore, the lack of a clear P-allocation pattern among leaf cells of chickpea may be due to low soil P availability. Many studies reporting differential cellular [P] in eudicot crops were grown under sufficient/excess P conditions; under such conditions, these crops may tend to accumulate 'surplus P' in epidermal cells, showing a preferential allocation of P to epidermal cells (Outlaw *et al.*, 1984; Conn and Gilliham 2010; Ding *et al.*, 2018a, b). This assumption can be explored by studying cellular P allocation in the leaves of chickpea supplied with varying P levels (including deficient, sufficient, and excess P). Combined with the results of P-allocation patterns in a

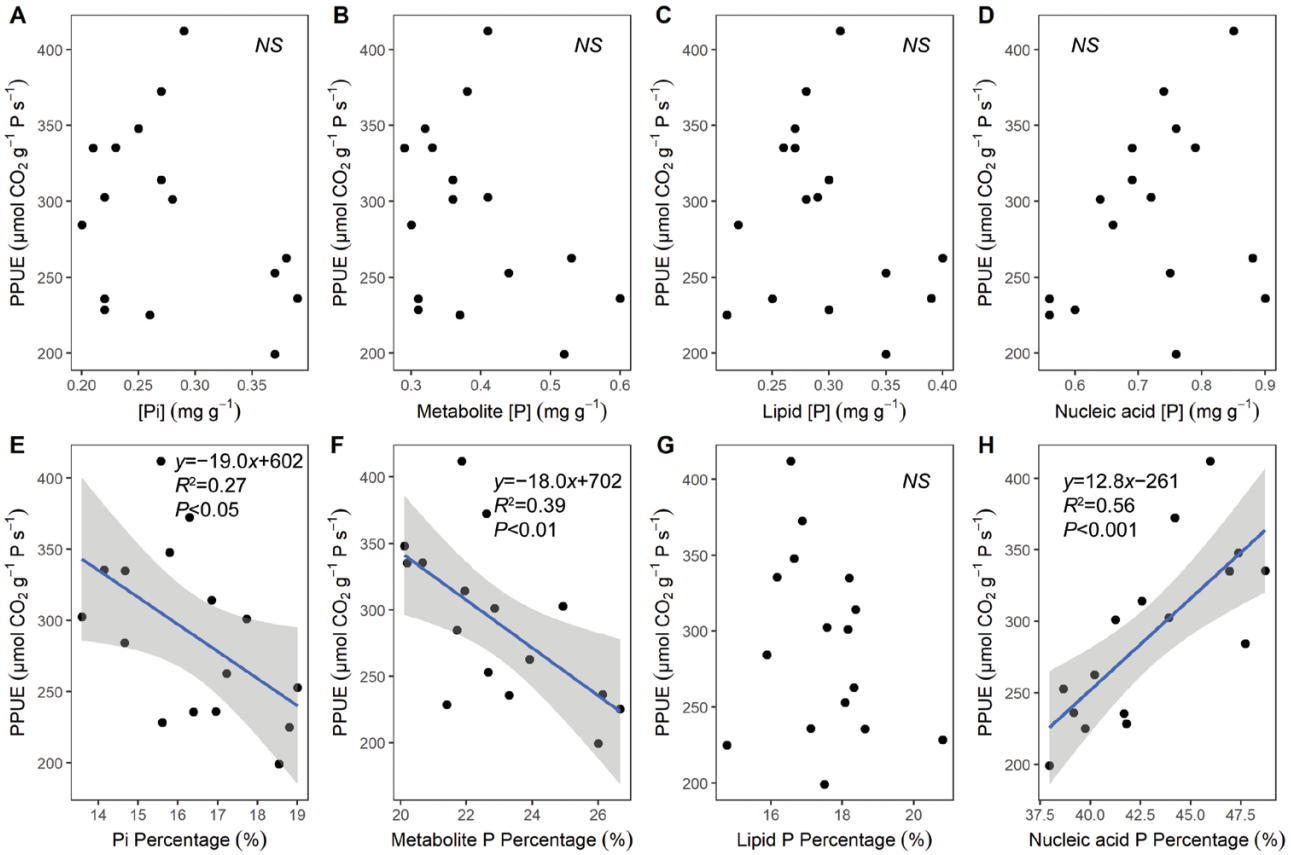

Fig. 6. Correlations between photosynthetic phosphorus use efficiency (PPUE) and concentration of each foliar phosphorus (P) fraction (A–D) or percentage of each foliar P fraction to total foliar P concentration ([P]) (E–H). Data are for four chickpea genotypes grown in soil with a low P supply; data points represent individual replicates (n=16). The regression analysis does not include the fraction of residual P, which showed extremely low concentrations and percentages compared with the other foliar P fractions. The shaded areas indicate the 95% confidence range derived from the models. NS, not significant; Pi, inorganic phosphate.

range of other eudicot species (Outlaw *et al.*, 1984; Storey and Leigh, 2004; Ding *et al.*, 2018a, b; Guilherme Pereira *et al.*, 2018; Hayes *et al.*, 2018, 2019), we suggest that eudicots show different allocation patterns of foliar P depending on species identity, specific evolutionary context, and P availability in growing environments, rather than following a single general pattern (Conn and Gilliham, 2010).

The accumulation of P has frequently been studied in conjunction with that of Ca, because the allocation of large amounts of both elements to the same cells would cause precipitation of calcium phosphate and result in both nutrients being unavailable (Leigh and Tomos, 1993; Williams *et al.*, 1993; McLaughlin and Wimmer, 1999; Karley *et al.*, 2000a; White and Broadley, 2003; Storey and Leigh, 2004; Hawkins *et al.*, 2008; Conn and Gilliham, 2010; Lambers, 2022). Allocation of P and Ca to distinct cell types has been reported in monocots and eudicots (Outlaw *et al.*, 1984; Treeby *et al.*, 1987; Leigh and Tomos, 1993; Williams *et al.*, 1993; Fricke *et al.*, 1994; Karley *et al.*, 2000a; Storey and Leigh, 2004; Conn and Gilliham, 2010). Generally, eudicots accumulate more Ca in mesophyll cells and P in epidermal cells (Outlaw *et al.*, 1984; Treeby *et al.*, 1987; Conn and Gilliham, 2010; Ding *et al.*, 2018a). Our results partly support this view, as all chickpea genotypes showed high [Ca] in their mesophyll, while [P] tended to be equal in mesophyll and epidermis. This implies that P co-existed with high [Ca] in mesophyll cells of chickpea. How could chickpea maintain such distribution patterns without incurring P and Ca deficiencies? There are two possible explanations. First, the cellular [P] in the mesophyll was probably too low to cause precipitation of Ca and P, due to the low soil P supply in the present study. Cellular [P] in the mesophyll is influenced by external P supply (Treeby *et al.*, 1987; Ding *et al.*, 2018b), with plants usually showing constitutive P- and Ca-allocation patterns at the species level (Guilherme Pereira *et al.*, 2018). Thus, it would be interesting to explore whether and how chickpea sustains the co-existence of P and Ca in mesophyll cells at a higher soil P availability. Second, despite P and high [Ca] being co-located in mesophyll cells, these elements likely occur in different subcellular compartments. Most of the P was present in various organic compounds (e.g. nucleic acids and phospholipids; Veneklaas *et al.*, 2012; Lambers, 2022). In

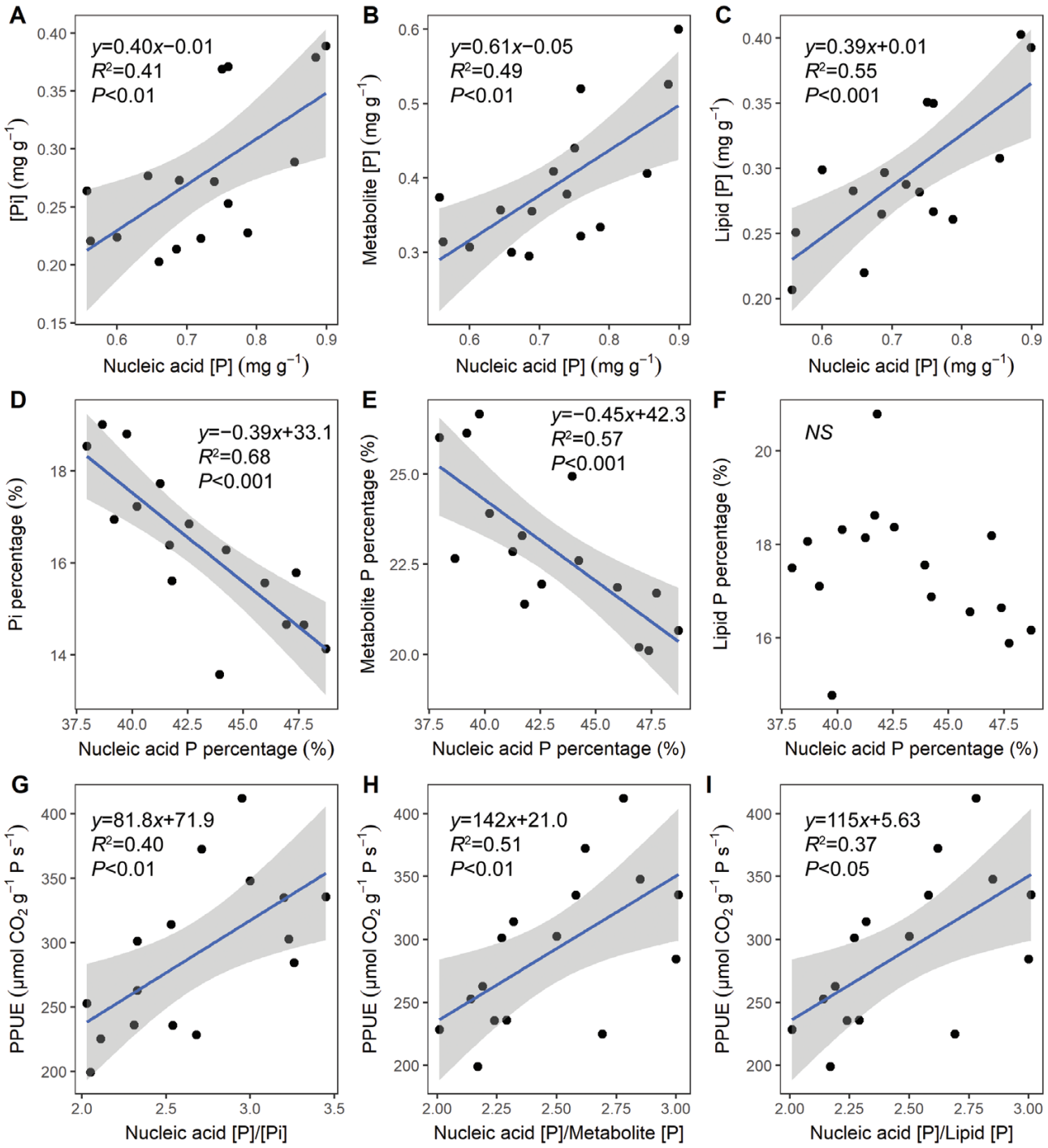

Fig. 7. Correlations between the nucleic acid phosphorus (P) and inorganic phosphate ([Pi]), metabolite P or lipid P expressed as concentrations (A–C) and percentages (D–F); and correlations between photosynthetic P use efficiency (PPUE) and the ratio of nucleic acid P to the other three foliar P fractions (G–I). Data are for four chickpea genotypes grown in soil with a low P supply; data points represent individual replicates (n=16). The regression analysis does not include the fraction of residual P, which showed extremely low concentrations and percentages compared with the other foliar P fractions. The shaded areas indicate the 95% confidence range derived from the models. NS, not significant.

contrast, foliar Pi is maintained at 20–30 mM within the cytosol (Mimura, 1995; Mimura *et al.*, 1996), whereas free Ca^{2+} is maintained in the cytosol in the submicromolar range due to its signaling roles (as secondary messenger), with variation above this range generally being toxic to cytosolic processes (Kirkby and Pilbeam, 1984; White and Broadley, 2003; McAinsh and Pittman, 2009; Conn and Gilliham, 2010). Most Ca is stored in the vacuole (up to 80 mM), acting as an

important counter-cation for various inorganic and organic anions (Conn and Gilliham, 2010). Overall, the mechanisms for the coexistence of Ca and P in the mesophyll remain unknown, but the high [Ca] in the mesophyll may partly explain why chickpea does not allocate more P to the mesophyll as we hypothesized (H1).

In summary, our results show that foliar cell-specific P allocation does not underlie the differences in PPUE among chickpea genotypes. Such knowledge extends our understanding of the linkage between the allocation patterns of foliar nutrients (P and Ca) and their physiological functions in eudicots. Further investigation of the subcellular distribution of P and Ca may yield exciting details on how these elements coexist and interact at the cellular level of vascular plants.

Does the allocation of foliar P fractions explain contrasting PPUE among chickpea genotypes?

As Pi and P-containing metabolites are required for various processes in photosynthesis (Veneklaas *et al.*, 2012; Dissanayaka *et al.*, 2021; Lambers, 2022), we hypothesized that optimized P allocation among foliar P fractions contribute to high PPUE in chickpea genotypes (H2, as shown in Fig. 1). In support of this hypothesis, we found that genotypes with high PPUE had lower total foliar [P] without compromising rapid photosynthetic rates, and the PPUE was tightly and negatively correlated with the percentages of Pi and metabolite P, indicating that a reduced relative allocation to Pi and metabolite P may confer high PPUE in chickpea genotypes. Remarkably, we also observed that reduced P allocation to Pi and metabolite P was associated with greater allocation to nucleic acid P, but not to lipid P. The association of a high PPUE with such a P-allocation pattern is explored below.

Maintaining a stable [Pi] and/or a large relative investment in metabolite P contributes to high PPUE at the species level (Hidaka and Kitayama, 2013; Sulpice *et al.*, 2014; Mo *et al.*, 2019; Zhang *et al.*, 2021). Inconsistent with these observations, we found that PPUE was negatively correlated with the percentage of Pi and metabolite P across the four chickpea genotypes. A similar negative correlation of PPUE with metabolite P has been found in rice (*Oryza sativa*; Hayes *et al.*, 2022). This divergence may be explained by a compensatory effect between a decrease in substrate concentration and an increase in catalytic efficiency. More specifically, Pi and P-containing metabolites are substrates for enzymes in a range of photosynthetic processes such as photophosphorylation and the Calvin–Benson cycle; a decrease in substrate concentration may curtail the activity of these reactions (Veneklaas *et al.*, 2012; Dissanayaka *et al.*, 2021; Lambers, 2022). To cope with decreased substrate concentrations and maintain a rapid metabolic flux, some plants may invest more in enzymes (i.e. enzyme concentrations), sustained by greater investment in nucleic acids (mainly rRNA) (Lambers, 2022). Supporting this contention, our results show that a lower relative investment in Pi and metabolite P was strongly associated with increased allocation of P to nucleic acids (Fig. 7). Similar trade-offs between the relative investments in metabolite P and nucleic acid P have been observed in subtropical forest species (Zhang *et al.*, 2018) and some native species from P-impoverished habitats in Mediterranean shrublands (Sulpice *et al.*, 2014; Yan *et al.*, 2019). For instance, despite these native species exhibiting low total foliar [P], the *Proteaceae* (e.g. *Hakea prostrata*) show low nucleic acid [P] and relatively high metabolite [P], whereas *Fabaceae* (e.g. *Acacia rostellifera*) show the opposite (Yan *et al.*, 2019). This suggests that even co-occurring species have evolved contrasting strategies for allocating leaf P fractions to cope with the evolutionary pressures of low soil P availability. Overall, to sustain high PPUE in chickpea, reduced P allocation to Pi and/or metabolite P (decreased substrate concentrations) may be compensated by a greater abundance of enzymes (indicated by increased investment to nucleic acid P, primarily rRNA). This provides novel insights into our understanding of how plants optimize P allocation to foliar P fractions for achieving a high PPUE at the genotype level. To capture the details of the interactions of nucleic acid P and metabolite P, further work is warranted to explore which metabolites and processes are affected and to what extent of the low allocation to Pi and/or metabolite P (i.e. a safe range in operation) could be compensated by increased investment in nucleic acid P/rRNA (increased synthesis of related enzymes).

Nucleic acids are the largest organic P fraction in leaves, and rRNA comprises the major component of this fraction, which is involved in protein synthesis (Dyer and Osborne, 1971; Veneklaas *et al.*, 2012; Raven, 2013b). We found that the high-PPUE chickpea genotypes tended to have a higher percentage of nucleic acid P (presumably mainly rRNA) than the low-PPUE genotypes. Similarly, Hayes *et al.* (2022) reported a positive correlation between PPUE and the percentage of nucleic acid P across five rice genotypes. However, this result differs from the observations on six *Proteaceae* species, showing that these species exhibited exceptionally high PPUE, while exhibiting low rRNA abundance in their mature leaves (Sulpice *et al.*, 2014). The mechanisms underlying contrasting P allocation patterns to nucleic acids in mature leaves among species or genotypes remain largely unknown (Han *et al.*, 2021; Hayes *et al.*, 2022; Lambers, 2022). Given that mature leaves have stopped growing, we surmise that the contrasting patterns in P allocation to nucleic acids are associated with distinct turnover rates of protein in these leaves among species or genotypes. Some species (e.g. chickpea in this study and rice in Hayes *et al.* (2022), which usually show relatively fast growth rates and shorter lifespans) tend to invest more P in nucleic acids (rRNA) in mature leaves, and this might allow those leaves to quickly replace damaged proteins by producing more abundant P-rich ribosomes and to respond rapidly to changing environments (Raven, 2013b; Nelson and Millar, 2015; Salih *et al.*, 2020; Lambers, 2022). In contrast, some species (e.g.

Proteaceae, which usually show relatively slow growth rates and longer lifespans) tend to exhibit low P investment in nucleic acids (rRNA) in their mature leaves. This allows them to decrease foliar P demand and use P in a more economical way, but it may also slow down the overall protein synthesis rate and restrict their response to changing environments (Sulpice *et al.*, 2014; Lambers, 2022). Therefore, there may be a trade-off between P use efficiency and leaf plasticity, when plants allocate more P to the nucleic acid fraction in mature leaves. Collectively, increased P allocation to nucleic acids (rRNA) in chickpea leaves may be associated with fast protein synthesis and turnover, e.g. the production of Rubisco and various Calvin–Benson cycle enzymes, and the replacement of damaged photosystem proteins (Nelson and Millar, 2015; Lambers, 2022), to sustain a rapid photosynthetic rate under low P conditions.

Reduced P investment in the lipid P fraction through lipid remodeling and/or replacement by lipids that do not contain P has been demonstrated as an important adaptation mechanism for plants to decrease overall foliar P demand, without compromising a relatively rapid photosynthetic rate at the species level (Lambers *et al.*, 2012; Hidaka and Kitayama, 2013) and genotype level (Jeong *et al.*, 2017; Han *et al.*, 2022; Hayes *et al.*, 2022). Inconsistent with this pattern, we found little difference in the concentration and percentage of lipid P among chickpea genotypes with contrasting PPUE, suggesting intraspecific variation in lipid P investment may not play a key role in determining PPUE among chickpea genotypes. Two possible explanations account for such divergence. First, phospholipids are important components of the endoplasmic reticulum and Golgi apparatus (e.g. endoplasmic reticulum accounts for >60% of the phospholipid mass in various cell types) (Lagace and Ridgway, 2013), all of which are needed for protein processing or modification (Hawes, 2005; Sun *et al.*, 2021). Considering that rapid synthesis of photosynthetic enzymes may occur in high-PPUE genotypes (as discussed above), these genotypes may maintain a greater amount of endoplasmic reticulum and Golgi apparatus to support rapid ribosomal protein synthesis rather than exhibit reduced investment. Second, low P allocation to phospholipids seems to be a species-specific response for plants to alleviate low-P stress. For instance, Mo *et al.* (2019) found that, in response to low P supply, plants showed distinct P-allocation patterns among foliar P fractions, including an increase, a decrease, or a slight change in lipid P allocation for different species.

Conclusions

This study explored the biochemical basis for high PPUE in chickpea genotypes under low soil P availability. We found that chickpea genotypes with high PPUE exhibited lower total foliar [P] without exhibiting slower photosynthetic rates. No consistent differences in cellular [P] occurred between photosynthetically active and inactive cells (i.e. mesophyll and epidermis), indicating foliar cell-specific P allocation did not account for differences in PPUE among chickpea genotypes. Furthermore, high PPUE was associated with reduced allocation to inorganic P and metabolite P, with PPUE being strongly and negatively correlated with the percentage of these two fractions. Finally, we demonstrated that reduced allocation to inorganic P and metabolite P was correlated with increased allocation to nucleic acid P, but not to lipid P. Overall, our findings suggest that optimized allocation to foliar P fractions, rather than preferential cell-specific P allocation, underlies high PPUE among chickpea genotypes. Greater P allocation to nucleic acids may be associated with faster protein synthesis and turnover to sustain a rapid photosynthetic rate under low P supply. This study enhances our fundamental understanding of how crop genotypes achieve a high PPUE under low P availability, and suggests fine-tuning of foliar P fractions as a promising strategy for chickpea breeding programs for simultaneously improving P efficiency and sustaining photosynthetic capacity.

Supplementary data

The following supplementary data are available at *JXB* online.

Fig. S1. The concentrations of foliar cell-specific potassium, magnesium, sulfur, and chlorine for four chickpea genotypes grown in soil with a low phosphorus supply.

Fig. S2. Representative anatomical schematics, secondary electron images, and qualitative element maps for four chickpea genotypes grown in soil with a low phosphorus supply.

Fig. S3. Correlations between the concentration of each foliar phosphorus (P) fraction and total foliar P concentration across four chickpea genotypes.

Table S1. Detailed information on four chickpea genotypes used in the experiment.

Table S2. Concentrations and percentages of each foliar phosphorus fraction for four chickpea genotypes grown in soil with a low phosphorus supply.

Table S3. Correlations between leaf photosynthetic rate and the concentrations of total leaf phosphorus (P) and each P fraction among four chickpea genotypes grown in soil with a low P supply.

Acknowledgements

We thank Rob Creasy and Bill Piasini for help with maintaining the plants in the glasshouse, and Dr Ruiting Gu for help with the harvest at The University of Western Australia. The authors acknowledge use of the facilities and technical assistance from Lyn Kirilak at Microscopy Australia at the Centre for Microscopy, Characterisation & Analysis, The University of Western Australia, a facility funded by the University, State and Commonwealth Governments.

Author contributions

ZW, JP, PC, MHR, KHMS, JS, and HL designed the study; ZW, XW, CG, ADB, and PC performed the experiment and collected the data; ZW, JP, PEH, PC, MHR, JS, and HL analysed and discussed the data; ZW led the writing of the manuscript. All authors contributed critically to the drafts and approved the final version for publication.

Conflict of interest

The authors declare that they have no conflicts of interest.

Funding

This work was funded by the National Natural Science Foundation of China (32130094 to JS, 32102471 to ZW), the China Postdoctoral Science Foundation (PC2021092 to ZW), and the Australian Research Council (LP200100341 to JP and HL).

Data availability

All data supporting the findings of this study are available from the corresponding authors upon request.

References

Bieleski RL. 1973. Phosphate pools, phosphate transport, and phosphate availability. Annual Review of Plant Biology **24**, 225–252.

Carstensen A, Herdean A, Schmidt SB, Sharma A, Spetea C, Pribil M, Husted S. 2018. The impacts of phosphorus deficiency on the photosynthetic electron transport chain. Plant Physiology **177**, 271–284.

Colwell JD. 1965. An automatic procedure for the determination of phosphorus in sodium hydrogen carbonate extracts of soils. Chemical Industry **21**, 893–895.

Cong WF, Suriyagoda LDB, Lambers H. 2020. Tightening the phosphorus cycle through phosphorus-efficient crop genotypes. Trends in Plant Science **25**, 967–975.

Conn S, Gilliham M. 2010. Comparative physiology of elemental distributions in plants. Annals of Botany **105**, 1081–1102.

de Mendiburu. 2017. Agricolae: statistical procedures for agricultural research. R package version 1:2-8. https://CRAN.R-project.org/package=agricolae

Denton MD, Veneklaas EJ, Freimoser FM, Lambers H. 2007. *Banksia* species (Proteaceae) from severely phosphorus-impoverished soils exhibit extreme efficiency in the use and re-mobilization of phosphorus. Plant, Cell & Environment **30**, 1557–1565.

Ding W, Clode PL, Clements JC, Lambers H. 2018a. Sensitivity of different *Lupinus* species to calcium under a low phosphorus supply. Plant, Cell & Environment **41**, 1512–1523.

Ding W, Clode PL, Clements JC, Lambers H. 2018b. Effects of calcium and its interaction with phosphorus on the nutrient status and growth of three *Lupinus* species. Physiologia Plantarum **163**, 386–398.

Dissanayaka D, Ghahremani M, Siebers M, Wasaki J, Plaxton WC. 2021. Recent insights into the metabolic adaptations of phosphorus-deprived plants. Journal of Experimental Botany **72**, 199–223.

Dyer TA, Osborne DJ. 1971. Leaf nucleic acids: II. Metabolism during senescence and the effect of kinetin. Journal of Experimental Botany **22**, 552–560.

Epstein E, Bloom AJ. 2005. Mineral nutrition of plants principles and perspectives. Sunderland, MA, USA: Sinauer Associates, Inc.

FAO. 2020. FAOSTAT. Rome: Food and Agriculture Organization of the United Nations. http://www.fao.org/faostat/en/

Fredeen AL, Raab TK, Rao IM, Terry N. 1990. Effects of phosphorus nutrition on photosynthesis in *Glycine max* (L.) Merr. Planta **181**, 399–405.

Fricke W, Leigh RA, Deri Tomos A. 1994. Concentrations of inorganic and organic solutes in extracts from individual epidermal, mesophyll and bundle-sheath cells of barley leaves. Planta **192**, 310–316.

Guilherme Pereira C, Clode PL, Oliveira RS, Lambers H. 2018. Eudicots from severely phosphorus-impoverished environments preferentially allocate phosphorus to their mesophyll. New Phytologist **218**, 959–973.

Halsted M, Lynch J. 1996. Phosphorus responses of C_3 and C_4 species. Journal of Experimental Botany **47**, 497–505.

Han Y, Hong W, Xiong C, Lambers H, Sun Y, Xu Z, Schulze WX, Cheng L. 2022. Combining analyses of metabolite profiles and phosphorus fractions to explore high phosphorus utilization efficiency in maize. Journal of Experimental Botany **73**, 4184–4203.

Han Z, Shi J, Pang J, Yan L, Finnegan PM, Lambers H. 2021. Foliar nutrient allocation patterns in *Banksia attenuata* and *Banksia sessilis* differing in growth rate and adaptation to low-phosphorus habitats. Annals of Botany **128**, 419–430.

Hawes C. 2005. Cell biology of the plant Golgi apparatus. New Phytologist **165**, 29–44.

Hawkins H-J, Hettasch H, Mesjasz-Przybylowicz J, Przybylowicz W, Cramer MD. 2008. Phosphorus toxicity in the Proteaceae: a problem in post-agricultural lands. Scientia Horticulturae **117**, 357–365.

Hayes PE, Adem GD, Pariasca-Tanaka J, Wissuwa M. 2022. Leaf phosphorus fractionation in rice to understand internal phosphorus-use efficiency. Annals of Botany **129**, 287–302.

Hayes PE, Clode PL, Guilherme Pereira C, Lambers H. 2019. Calcium modulates leaf cell-specific phosphorus allocation in Proteaceae from south-western Australia. Journal of Experimental Botany **70**, 3995–4009.

Hayes PE, Clode PL, Oliveira RS, Lambers H. 2018. Proteaceae from phosphorus-impoverished habitats preferentially allocate phosphorus to photosynthetic cells: An adaptation improving phosphorus-use efficiency. Plant, Cell & Environment **41**, 605–619.

Hayes PE, Nge FJ, Cramer MD, *et al*. 2021. Traits related to efficient acquisition and use of phosphorus promote diversification in Proteaceae in phosphorus-impoverished landscapes. Plant and Soil **462**, 67–88.

Heanes DL. 1984. Determination of total organic-C in soils by an improved chromic acid digestion and spectrophotometric procedure. Communications in Soil Science and Plant Analysis **15**, 1191–1213.

Hidaka A, Kitayama K. 2013. Relationship between photosynthetic phosphorus-use efficiency and foliar phosphorus fractions in tropical tree species. Ecology and Evolution **3**, 4872–4880.

Hodson MJ, Sangster AG. 1988. Observations on the distribution of mineral elements in the leaf of wheat (*Triticum aestivum* L.), with particular reference to silicon. Annals of Botany **62**, 463–471.

Hurley BA, Tran HT, Marty NJ, Park J, Snedden WA, Mullen RT, Plaxton WC. 2010. The dual-targeted purple acid phosphatase isozyme AtPAP26 is essential for efficient acclimation of Arabidopsis to nutritional phosphate deprivation. Plant Physiology **153**, 1112–1122.

Jeong K, Julia CC, Waters DLE, Pantoja O, Wissuwa M, Heuer S, Liu L, Rose TJ. 2017. Remobilisation of phosphorus fractions in rice flag leaves during grain filling: implications for photosynthesis and grain yields. PLoS One **12**, e0187521.

Jukanti AK, Gaur PM, Gowda CLL, Chibbar RN. 2012. Nutritional quality and health benefits of chickpea (*Cicer arietinum* L.): a review. British Journal of Nutrition **108**, S11–S26.

Karley AJ, Leigh RA, Sanders D. 2000a. Differential ion accumulation and ion fluxes in the mesophyll and epidermis of barley. Plant Physiology **122**, 835–844.

Karley AJ, Leigh RA, Sanders D. 2000b. Where do all the ions go? The cellular basis of differential ion accumulation in leaf cells. Trends in Plant Science **5**, 465–470.

Kedrowski RA. 1983. Extraction and analysis of nitrogen, phosphorus and carbon fractions in plant-material. Journal of Plant Nutrition **6**, 989–1011.

Kirkby EA, Pilbeam DJ. 1984. Calcium as a plant nutrient. Plant, Cell & Environment **7**, 397–405.

Lagace TA, Ridgway ND. 2013. The role of phospholipids in the biological activity and structure of the endoplasmic reticulum. Biochimica Biophysica Acta **1833**, 2499–2510.

Lambers H. 2022. Phosphorus acquisition and utilization in plants. Annual Review of Plant Biology **73**, 17–42.

Lambers H, Cawthray GR, Giavalisco P, Kuo J, Laliberte E, Pearse SJ, Scheible WR, Stitt M, Teste F, Turner BL. 2012. Proteaceae from severely phosphorus-impoverished soils extensively replace phospholipids with galactolipids and sulfolipids during leaf development to achieve a high photosynthetic phosphorus-use-efficiency. New Phytologist **196**, 1098–1108.

Lambers H, Clode PL, Hawkins H-J, Laliberté E, Oliveira RS, Reddell P, Shane MW, Stitt M, Weston P. 2015. Metabolic adaptations of the non-mycotrophic proteaceae to soils with low phosphorus availability. Annual Plant Reviews **48**, 289–335.

Leigh RA, Tomos AD. 1993. Ion distribution in cereal leaves: pathways and mechanisms. Philosophical Transactions of the Royal Society of London, Series B: Biological Sciences **341**, 75–86.

Liao H, Yan X. 1999. Seed size is closely related to phosphorus use efficiency and photosynthetic phosphorus use efficiency in common bean. Journal of Plant Nutrition **22**, 877–888.

Lim S-L, Flütsch S, Liu J, Distefano L, Santelia D, Lim BL. 2022. *Arabidopsis* guard cell chloroplasts import cytosolic ATP for starch turnover and stomatal opening. Nature Communications **13**, 652.

McAinsh MR, Pittman JK. 2009. Shaping the calcium signature. New Phytologist **181**, 275–294.

McCully ME, Canny MJ, Huang CX, Miller C, Brink F. 2010. Cryo-scanning electron microscopy (CSEM) in the advancement of functional plant biology: energy dispersive X-ray microanalysis (CEDX) applications. Functional Plant Biology **37**, 1011–1040.

McLaughlin SB, Wimmer R. 1999. Calcium physiology and terrestrial ecosystem processes. New Phytologist **142**, 373–417.

Mimura T. 1995. Homeostasis and transport of inorganic phosphate in plants. Plant and Cell Physiology **36**, 1–7.

Mimura T, Sakano K, Shimmen T. 1996. Studies on the distribution, re-translocation and homeostasis of inorganic phosphate in barley leaves. Plant, Cell & Environment **19**, 311–320.

Mo Q, Za L, Sayer EJ, Lambers H, Li Y, Zou B, Tang J, Heskel M, Ding Y, Wang F. 2019. Foliar phosphorus fractions reveal how tropical plants maintain photosynthetic rates despite low soil phosphorus availability. Functional Ecology **33**, 503–513.

Motomizu S, Wakimoto T, Tôei K. 1983. Spectrophotometric determination of phosphate in river waters with molybdate and malachite green. Analyst **108**, 361–367.

Nakamura Y. 2017. Plant phospholipid diversity: emerging functions in metabolism and protein–lipid interactions. Trends in Plant Science **22**, 1027–1040.

Nakamura Y, Koizumi R, Shui G, Shimojima M, Wenk MR, Ito T, Ohta H. 2009. *Arabidopsis* lipins mediate eukaryotic pathway of lipid metabolism and cope critically with phosphate starvation. Proceedings of the National Academy of Sciences, USA **106**, 20978–20983.

Nelson CJ, Millar AH. 2015. Protein turnover in plant biology. Nature Plants **1**, 15017.

Outlaw WH Jr, Tarczynski MC, Miller WI. 1984. Histological compartmentation of phosphate in *Vicia faba* L. leaflet: possible significance to stomatal functioning. Plant Physiology **74**, 430–433.

Pang J, Zhao H, Bansal R, Bohuon E, Lambers H, Ryan MH, Siddique KHM. 2018. Leaf transpiration plays a role in phosphorus acquisition among a large set of chickpea genotypes. Plant, Cell & Environment **41**, 2069–2079.

Pinheiro, J, Bates D. 2000. Mixed-effects models in S and S-PLUS. New York: Springer New York.

Plaxton WC, Tran HT. 2011. Metabolic adaptations of phosphate-starved plants. Plant Physiology **156**, 1006–1015.

Raven JA. 2013a. The evolution of autotrophy in relation to phosphorus requirement. Journal of Experimental Botany **64**, 4023–4046.

Raven JA. 2013b. RNA function and phosphorus use by photosynthetic organisms. Fronters in Plant Science **4**, 536.

Rayment GE, Higginson FR. 1992. Australian laboratory handbook of soil and water chemical methods. Melbourne: Inkata Press.

R Development Core Team. 2022. R: a language and environment forstatistical computing. Vienna, Austria: R Foundation for Statistical Computing. https://www.R-project.org

Salih KJ, Duncan O, Li L, O'Leary B, Fenske R, Trosch J, Millar AH. 2020. Impact of oxidative stress on the function, abundance, and turnover of the Arabidopsis 80S cytosolic ribosome. The Plant Journal **103**, 128–139.

Schachtman DP, Reid RJ, Ayling SM. 1998. Phosphorus uptake by plants: from soil to cell. Plant Physiology **116**, 447–453.

Shane MW, McCully ME, Lambers H. 2004. Tissue and cellular phosphorus storage during development of phosphorus toxicity in *Hakea prostrata* (Proteaceae). Journal of Experimental Botany **55**, 1033–1044.

Shen J, Yuan L, Zhang J, Li H, Bai Z, Chen X, Zhang W, Zhang F. 2011. Phosphorus dynamics: from soil to plant. Plant Physiology **156**, 997–1005.

Sibbesen E. 1978. An investigation of the anion-exchange resin method for soil phosphate extraction. Plant and Soil **50**, 305–321.

Srinivasarao C, Ganeshamurthy AN, Ali M, Venkateswarlu B. 2006. Phosphorus and micronutrient nutrition of chickpea genotypes in a multi-nutrient-deficient typic ustochrept. Journal of Plant Nutrition **29**, 747–763.

Stitt M, Lunn J, Usadel B. 2010. Arabidopsis and primary photosynthetic metabolism – more than the icing on the cake. The Plant Journal **61**, 1067–1091.

Storey R, Leigh RA. 2004. Processes modulating calcium distribution in citrus leaves. An investigation using x-ray microanalysis with strontium as a tracer. Plant Physiology **136**, 3838–3848.

Sulpice R, Ishihara H, Schlereth A, *et al*. 2014. Low levels of ribosomal RNA partly account for the very high photosynthetic phosphorus-use efficiency of Proteaceae species. Plant, Cell & Environment **37**, 1276–1298.

Sun J, Li J, Wang M, Song Z, Liu J. 2021. Protein quality control in plant organelles: current progress and future perspectives. Molecular Plant **14**, 95–114.

Suriyagoda LDB, Ryan MH, Gille CE, Dayrell RLC, Finnegan PM, Ranathunge K, Nicol D, Lambers H. 2023. Phosphorus fractions in leaves. New Phytologist, doi: 10.1111/nph.18588.

Tawaraya K, Honda S, Cheng W, Chuba M, Okazaki Y, Saito K, Oikawa A, Maruyama H, Wasaki J, Wagatsuma T. 2018. Ancient rice cultivar extensively replaces phospholipids with non-phosphorus glycolipid under phosphorus deficiency. Physiologia Plantarum **163**, 297–305.

Tjellstrom H, Andersson MX, Larsson KE, Sandelius AS. 2008. Membrane phospholipids as a phosphate reserve: the dynamic nature of phospholipid-to-digalactosyl diacylglycerol exchange in higher plants. Plant, Cell & Environment **31**, 1388–1398.

Treeby MT, van Steveninck RF, de Vries HM. 1987. Quantitative estimates of phosphorus concentrations within *Lupinus luteus* leaflets by means of electron probe X-ray microanalysis. Plant Physiology **85**, 331–334.

Tsujii Y, Oikawa M, Kitayama K. 2017. Significance of the localization of phosphorus among tissues on a cross-section of leaf lamina of Bornean tree species for phosphorus-use efficiency. Journal of Tropical Ecology **33**, 237–240.

Varshney RK, Thudi M, Roorkiwal M, *et al*. 2019. Resequencing of 429 chickpea accessions from 45 countries provides insights into genome diversity, domestication and agronomic traits. Nature Genetics **51**, 857–864.

Veneklaas EJ, Lambers H, Bragg J, *et al*. 2012. Opportunities for improving phosphorus-use efficiency in crop plants. New Phytologist **195**, 306–320.

Vitousek PM, Porder S, Houlton BZ, Chadwick OA. 2010. Terrestrial phosphorus limitation: mechanisms, implications, and nitrogen–phosphorus interactions. Ecological Applications **20**, 5–15.

Warren CR. 2011. How does P affect photosynthesis and metabolite profiles of *Eucalyptus globulus*? Tree Physiology **31**, 727–739.

White PJ, Broadley MR. 2003. Calcium in plants. Annals of Botany **92**, 487–511.

Williams ML, Thomas BJ, Farrar JF, Pollock CJ. 1993. Visualizing the distribution of elements within barley leaves by energy dispersive X-ray image maps (EDX maps). New Phytologist **125**, 367–372.

Wright IJ, Reich PB, Westoby M, *et al*. 2004. The worldwide leaf economics spectrum. Nature **428**, 821–827.

Yan L, Zhang X, Han Z, Pang J, Lambers H, Finnegan PM. 2019. Responses of foliar phosphorus fractions to soil age are diverse along a 2 Myr dune chronosequence. New Phytologist **223**, 1621–1633.

Ye D, Clode P, Hammer TA, Pang J, Lambers H, Ryan M. 2021. Accumulation of phosphorus and calcium in different cells protects the phosphorus-hyperaccumulator *Ptilotus exaltatus* from phosphorus toxicity in high-phosphorus soils. Chemosphere **264**, 12.

Zhang G, Zhang L, Wen D. 2018. Photosynthesis of subtropical forest species from different successional status in relation to foliar nutrients and phosphorus fractions. Scientific Reports **8**, 10455.

Zhang L, Luo X, Lambers H, Zhang G, Liu N, Zang X, Xiao M, Wen D. 2021. Effects of elevated CO_2 concentration and nitrogen addition on foliar phosphorus fractions of *Mikania micranatha* and *Chromolaena odorata* under low phosphorus availability. Physiologia Plantarum **173**, 2068–2080.